

Supplementary Information for

Synaptic Plasticity Realized by Selective Oxidation of TiS₃ Nanosheet for Neuromorphic Devices

Jing-Kai Qin^a, Hai-Lin Sun^a, Pei-Yu Huang^a, Yang Li^b, Liang Zhen^{a, b}, Cheng-Yan Xu^{a, b*}

^a Sauvage Laboratory for Smart Materials, School of Materials Science and Engineering,
Harbin Institute of Technology (Shenzhen), Shenzhen 518055, China

^b MOE Key Laboratory of Micro-Systems and Micro-Structures Manufacturing, Harbin
Institute of Technology, Harbin 150080, China

*E-mail addresses: cy_xu@hit.edu.cn

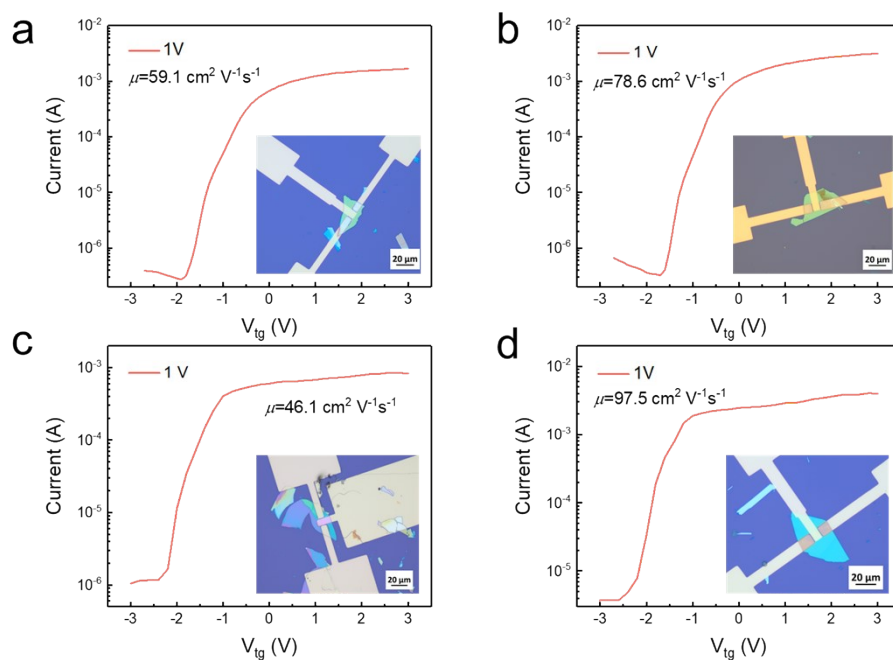


Figure S1. Photograph and transfer curves of typical device with mobility of (a) $59.1 \text{ cm}^2 \text{ V}^{-1} \text{ s}^{-1}$, (b) $78.6 \text{ cm}^2 \text{ V}^{-1} \text{ s}^{-1}$, (c) $46.1 \text{ cm}^2 \text{ V}^{-1} \text{ s}^{-1}$, (d) $97.5 \text{ cm}^2 \text{ V}^{-1} \text{ s}^{-1}$.

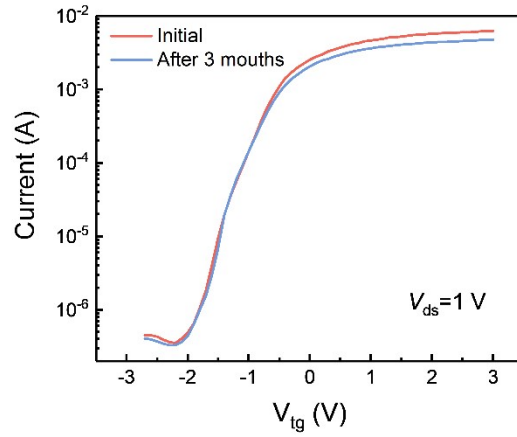


Figure S2. The environmental stability of TiS_3 field-effect transistor after exposure to air for 3 months.

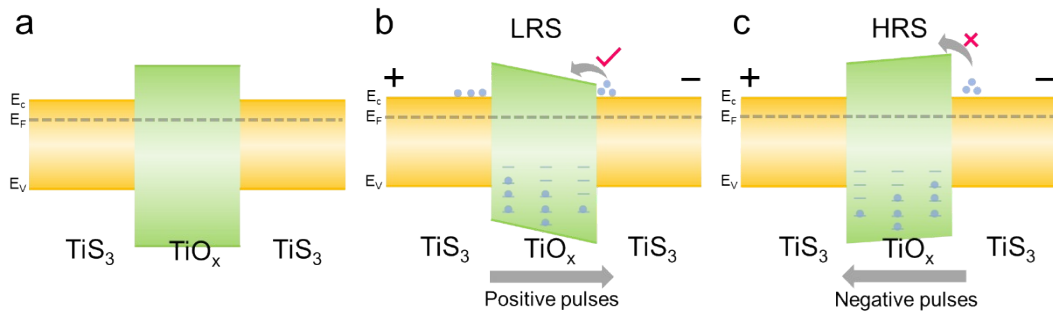


Figure S3. The energy band diagram of $\text{TiS}_3\text{-TiO}_x\text{-TiS}_3$ heterostructures (a) in initial state, (b) in LRS programmed by positive pulses, (c) in HRS programmed by negative pulses.

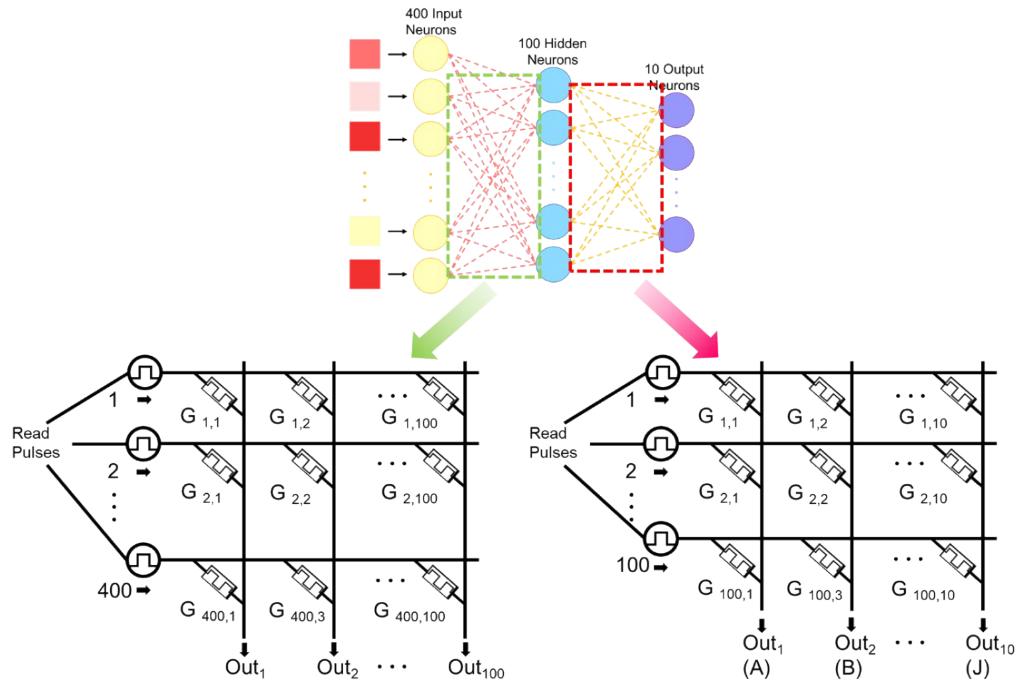


Figure S4. The corresponding schematic device array structure of ANN.